remote sensing

MDPI

Article

Assessment of Habitat Suitability for *Oedaleus decorus asiaticus* Using MaxEnt and Frequency Ratio Model in Xilingol League, China

Raza Ahmed [1,2], Wenjiang Huang [1,2,*], Yingying Dong [1,2], Jing Guo [1,2], Zeenat Dildar [1,2], Zahid Ur Rahman [1,2,3], Yan Zhang [1,2], Xianwei Zhang [1,4], Bobo Du [5] and Fangzheng Yue [6]

1 Key Laboratory of Remote Sensing and Digital Earth, Aerospace Information Research Institute, Chinese Academy of Sciences, Beijing 100101, China; razaahmed3550@mails.ucas.ac.cn (R.A.); dongyy@aircas.ac.cn (Y.D.); guojing211@mails.ucas.ac.cn (J.G.); zeenatdildar123@mails.ucas.ac.cn (Z.D.); 31192048@mails.ucas.ac.cn (Z.U.R.); zhangyan236@mails.ucas.ac.cn (Y.Z.); 107556520131@stu.xju.edu.cn (X.Z.)
2 University of Chinese Academy of Sciences, Beijing 100049, China
3 International Research Center of Big Data for Sustainable Development Goals (CBAS), Beijing 100094, China
4 College of Geography, Remote Sensing Sciences Xinjiang University, Urumqi 830046, China
5 Key Laboratory of Biohazard Monitoring and Green Prevention and Control in Artificial Grassland, Ministry of Agriculture and Rural Affairs, Hohhot 010010, China; dubobo@caas.cn
6 Center for Biological Disaster Prevention and Control, National Forestry and Grassland Administration, Shenyang 110034, China; yuefangzheng@nfga.gov.cn
* Correspondence: huangwj@aircas.ac.cn

Abstract: Grasshoppers can significantly disrupt agricultural and livestock management because they reproduce and develop quickly in friendly environments. Xilingol League is the region most severely affected by grasshopper infestations. The region's extensive grasslands are considered valuable, a critical component of the local ecosystem, a vital resource for the region's key economic activity of livestock farming, and crucial for supporting diverse flora and fauna, carbon sequestration, and climate regulation. *Oedaleus decorus asiaticus* (*O. d. asiaticus*) is highly harmful in Xilingol League in the Inner Mongolia Autonomous Region of China. Therefore, early warning is crucial for projecting *O. d. asiaticus's* regional spread and detecting the impacts of critical environmental elements. We systematically identified 26 major contributing elements by examining four categories of environmental factors— meteorology, vegetation, soil, and topography—encompassing the three growth phases of grasshoppers. Furthermore, the MaxEnt and frequency ratio (FR) approaches, coupled with multisource remote sensing data, were used to predict a potentially appropriate distribution (habitat suitability) of *O. d. asiaticus* in Xilingol League. The research found nine key habitat factors influencing *O. d. asiaticus* distribution: the mean specific humidity during the adult stage (ASH), vegetation type (VT), aboveground biomass during the nymph stage (NAB), soil sand content (SSAND), mean precipitation during the egg stage (EP), mean precipitation during the nymph stage (NP), soil bulk density (SBD), elevation, and soil type (ST). Additionally, our analysis revealed that the most suitable and moderately suitable habitats for *O. d. asiaticus* are predominantly located in the southern and eastern parts of Xilingol League, with significant concentrations in West Ujumqin, East Ujumqin, Xilinhot, Zhenglan, Zheng Xiangbai, Duolun, and Taipusi. Based on the suitable habitat results, policymakers may make judgments about future management actions to preserve the ecological security of grasslands and their sustainable growth. This study indicates that the Maxent approach exhibited superior accuracy (receiver operating characteristic) compared to the FR approach for assessing the habitat suitability for *O. d. asiaticus* in Xilingol League.

Academic Editor: Michele Innangi

Received: 30 December 2024
Revised: 26 February 2025
Accepted: 26 February 2025
Published: 27 February 2025

Citation: Ahmed, R.; Huang, W.; Dong, Y.; Guo, J.; Dildar, Z.; Rahman, Z.U.; Zhang, Y.; Zhang, X.; Du, B.; Yue, F. Assessment of Habitat Suitability for *Oedaleus decorus asiaticus* Using MaxEnt and Frequency Ratio Model in Xilingol League, China. *Remote Sens.* **2025**, *17*, 846. https://doi.org/10.3390/rs17050846

Copyright: © 2025 by the authors. Submitted for possible open access publication under the terms and conditions of the Creative Commons Attribution (CC BY) license (https://creativecommons.org/licenses/by/4.0/).

Keywords: grasshopper; MaxEnt; frequency ratio (FR) approach; habitat suitability; key habitat factors

1. Introduction

Xilingol League in the Inner Mongolia Autonomous Region has a highly concentrated population of *Oedaleus decorus asiaticus* (*O. d. asiaticus*), which often affects the ecosystems across the northern part of China [1]. In the interim, an infestation of grasshoppers results in significant ecological and economic repercussions, including prairie loss and dryness [2–4]. Consequently, managing *O. d. asiaticus* is essential for establishing natural grasslands and maintaining the excellent state of grass ecosystems, which are vital for sustaining herbivorous fauna. This remarkable grasshopper species falls under the Orthoptera category and is a member of the family *Oedipodidae* [5]. Members of the family *Oedipodidae* severely impact many plant species, including *Stipa* and *Leymus chinesis* [6,7]. Managing members of the family *Oedipodidae* becomes exceedingly challenging when swarming commences collective behavior due to their rapid growth in number, damaging capacity, and remote dispersal potential [8]. Chemical treatments have long been the standard for grasshopper control, but this approach can potentially harm the ecosystem and is not sustainable in the long run [9]. Precise outbreak prediction and management are crucial for reducing dependence on chemical pesticides. Our study leverages the MaxEnt and FR approaches, remote sensing data, and *O. d. asiaticus* presence data to predict potential outbreak locations more accurately. This precision can facilitate early intervention treatments that are more localized and less reliant on chemical pesticides, thereby reducing overall chemical usage and environmental impact [10]. Grasshopper infestations pose a significant problem in Inner Mongolia, affecting approximately 600 thousand hectares of land annually. The species diversity in the meadow steppe of Xilingol League typically ranges from 10 to 15 species per square meter [11]. Consequently, accurately assessing the environmental suitability for these grasshopper species in Xilingol League is critical. This assessment is essential for devising strategies to mitigate the effects of potential future outbreaks [12]. The traditional method for identifying possible locations of grasshopper outbreaks entails the human compilation of field data, which takes a long time and is labor intensive [13]. Furthermore, grasshoppers flourish in distant and challenging terrains that are difficult to access [14]. Nonetheless, relevant data with exact geographical and temporal resolutions are now much easier to obtain because of the development of remote sensing technology [15]. Integrating remote sensing with a geographic information system (GIS) and ecological data is a robust method for identifying potential grasshopper outbreak locations [16].

This combined approach leverages the advantages of remote sensing to monitor environmental conditions and patterns that indicate the locations of pest outbreaks, thereby enhancing our predictive capabilities and response to potential outbreaks across large areas [17]. Prior research has determined a close and intricate connection between the presence of locusts and a range of ecological parameters [18,19]. Habitat elements such as meteorological conditions, topography, properties of the soil, and vegetation affect the development and maturation of grasshoppers [20–25]. Precipitation and temperature are the key meteorological elements that primarily influence grasshoppers [26–29]. Temperature impacts the occurrence of grasshoppers by influencing their development, survival, and reproduction [30]. This is because warmer temperatures expedite the hatching of grasshopper eggs and alleviate the adverse effects of drought [31]. In addition, temperature variations impact the availability of suitable habitats for grasshoppers and shift the assemblage of grasshoppers [32]. Precipitation, which affects soil moisture, primarily

influences the development of grasshoppers [33]. The topography, including altitude, position, slope, and landscape variety, indirectly affects grasshoppers' movement and population size by modifying variations in precipitation, light, and temperature [23,34–37]. Additionally, soil's physical and chemical characteristics, including texture, moisture, pH, salinity, etc., affect the life cycle of grasshoppers [38,39]. The presence of grasshoppers indicates a strong association with the presence of plants [36]. The specific composition of plants in a given area and the extent of vegetation coverage directly impact the growth and maturation of grasshoppers [40,41]. As previous research has shown, many habitat conditions influence the presence of grasshoppers [42]. Hence, it is imperative to establish the correlation between the presence of grasshoppers and the specific environmental conditions of the location [43].

Species distribution models (SDMs) are crucial for determining suitable habitats for grasshoppers [11]. A species distribution model is a mathematical technique to accurately estimate unknown distributions using limited data [44]. Techniques such as BIOCLIM, DOMAIN, random forest (RF), the generalized linear model (GLM), support vector machine (SVM), GARP, and the maximum entropy model (the MaxEnt approach) are examples of SDM methods that are extensively utilized [45,46]. The MaxEnt approach is effective at modeling species niches despite a limited amount of occurrence data [47]. Furthermore, the MaxEnt approach can effectively analyze and measure habitat parameters [1]. Therefore, we can assess and predict the locations of suitable grasshopper habitats by using the MaxEnt approach in conjunction with remote sensing data and vital habitat parameters [8].

The frequency ratio (FR) approach is a widely accepted technique for accurately assessing potential hazards [48]. The FR approach is a statistical framework that assesses the significance of each component category for every variable and analyzes its influence on the incidence of disasters [49,50]. Numerous academic fields, such as geosciences, hazard and disaster management, and environmental sciences, extensively use the FR approach [51,52].

The MaxEnt and FR approaches, along with remote sensing data from various sources and *O. d. asiaticus* presence data within Xilingol, formed the foundation of our research. This study has four main objectives: 1. To determine the spatial distribution of the grasshopper species *Oedaleus decorus asiaticus* (Bei-Bienko) in the Xilingol region. 2. To investigate the influence of habitat factors on the distribution of *O. d. asiaticus* and determine their relative contributions. 3. To evaluate the predictive capabilities of the MaxEnt and FR approaches when identifying suitable habitats for *O. d. asiaticus*. 4. To describe the areas in Xilingol that are suitable for *O. d. asiaticus*. This research's main innovation is the first-ever creation of a grasshopper habitat suitability map in Inner Mongolia's Xilingol region using a GIS-based frequency ratio (FR) approach. The results of this study may help administrators and decision makers in the prediction of *O. d. asiaticus* disasters in advance.

2. Materials and Methods

2.1. Study Area

This study selected Xilingol League (44° 56′ 40.92″N, 115° 22′ 44.40″E) as the study area (Figure 1A). Xilingol League, which covers 200,000 km^2, consists of two county-level cities, one county, nine banners, and one administrative management district [53]. Figure 1B illustrates that the occurrence points for *O. d. asiaticus* were specifically collected from areas within Xilingol League that experienced damage in 2022. The region's climate is characterized by an annual rainfall of 288 mm, pan evaporation levels between 1700 to 2600 mm, and a mean annual temperature of 3.60 °C, with temperatures ranging from a low of −20 °C in January to a high of 21 °C in July [54]. The vegetation spectrum of the

study area is diverse, including grassland, agricultural, meadow, thicket, and forest formations, with grassland vegetation being the predominant land cover type, constituting 90% of the total area, as illustrated in Figure 1C. Forests cover an additional 5860 square kilometers, representing 2.9% of the area [55]. In the research region, the principal geomorphological categories are castanozem, meadow soil, and chernozem, all of which are favorable to grasshopper reproduction [56]. *Leymus chinensis*, the predominant grass species, exhibits robust growth potential. *Achnatherum sibiricum* and *Stipa grandis*, which grasshoppers more frequently consume, also rank among the top-growing grasses in the region [57].

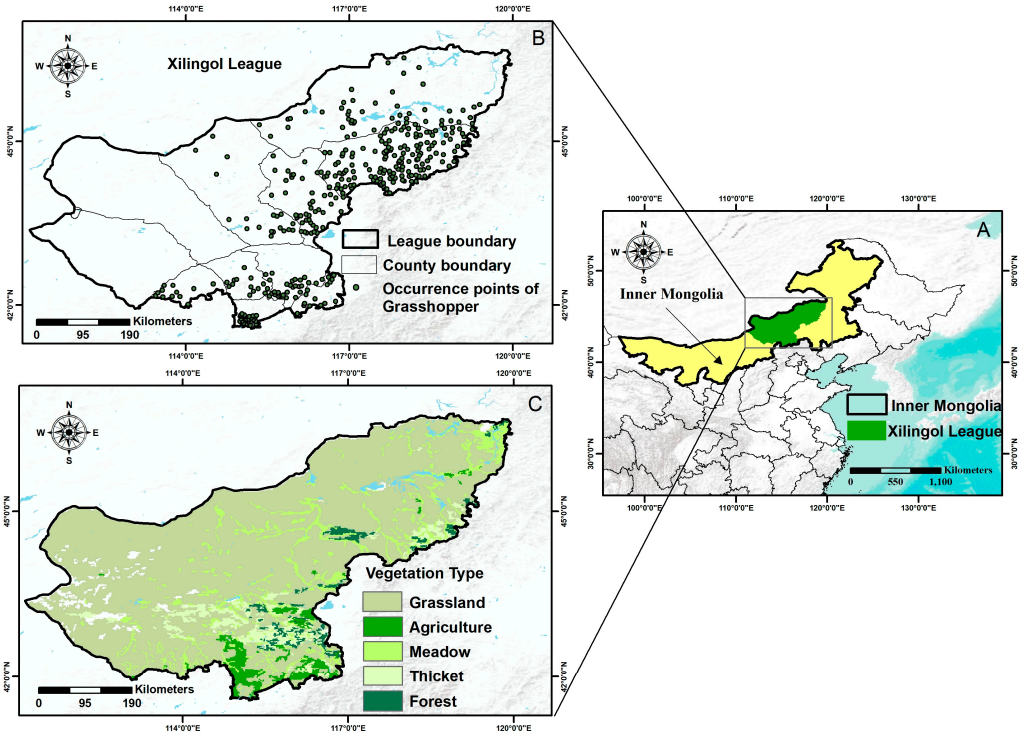


Figure 1. (**A**) Location of the study area; (**B**) Grasshopper occurrence points in the study area; (**C**) Vegetation types in the study area.

2.2. Data Acquisition and Processing

2.2.1. Satellite Data

We conducted this study using the Google Earth Engine (GEE) and utilized MODIS products MOD09A1.061, MOD11A1.061, and MOD13A2.061 to collect soil salinity index, land surface temperature, and normalized difference vegetation index data. The dataset utilized in this study comprises averaged raster data collected across the year 2022, with calculations tailored to the developmental stages of the grasshopper. The mean land surface temperature (LST) data had a spatial resolution of 1 km and a temporal resolution of 1 day. The soil salinity index (SI) data had a spatial resolution of 1 km and a temporal resolution of 8 days, while the normalized difference vegetation index (NDVI) data had a spatial resolution of 1 km and a temporal resolution of 16 days.

To evaluate vegetation growth, we used NDVI data from the MOD13A2.061 product within the Google Earth Engine (GEE) to estimate surface biomass, applying a specific formula for this purpose [58]:

$$AB = 26.38e^{3.8725 \times NDVI} \quad (1)$$

In addition, this study took into account the impact of the soil salinity index (SI) while choosing remote sensing data in the green light band "sur_refl_b04" and the red light band "sur_refl_b01," as specified in Equation (2) [59]. The bands depicted in the data represent the soil salinity index levels in the grasshoppers' subterranean habitat, encompassing information for their egg, nymph, and adult phases.

$$SI = \sqrt{B_g \times B_r} \quad (2)$$

In the above formula, B_r denotes the red band, whereas B_g denotes the green band.

2.2.2. Meteorological Data

We collected precipitation, soil moisture, and specific humidity data for the year 2022 from the GPM v6 dataset and the FLDAS (Famine Early Warning Systems Network (FEWSNET) Land Data Assimilation System) dataset, respectively, for the three and two developmental stages. The specific humidity, soil moisture, and precipitation data had a spatial resolution of 11,132 m. The precipitation and soil moisture data had a temporal resolution of 1 month, and the specific humidity data had a temporal resolution of 1 day.

2.2.3. Soil and Other Geospatial Data

We obtained data on soil sand, soil organic carbon, soil silt, soil bulk density, soil nitrogen (5–15 cm), soil pH (5–15 cm), and soil clay content (5–15 cm) from Soilgrids 250 m (https://www.soilgrids.org). We acquired the vegetation type and soil type data from the 1:1,000,000 national database, last updated in 2015. We retrieved the topography data from the Chinese Academy of Sciences Geospatial Data Cloud. The Google Earth Engine was used to download and compute all satellite, meteorological, soil, and topographic data. After completing the pre-processing steps of mosaicking, masking, and re-projection, we resampled all of the data to a spatial resolution of one kilometer.

2.2.4. Field Survey Data

The Xilingol region's grassland pest control stations provided the survey data for this study, which covered the year 2022 (Figure 1). Field surveys were conducted between 09:00 and 17:00 on sunny days, during the nymph and adult stages of *O. d. asiaticus* (from May to July) within the study area. A total of 400 occurrence points were recorded during these surveys. The surveys followed a regional approach, adhering to the agriculture industry standards of the People's Republic of China (NY/T 1578-2007, Guidelines on grasshopper and locality investments in grasslands), to thoroughly assess grasshopper presence. We conducted a comprehensive multipoint survey along the entire route, covering all major natural geomorphic units and sites where grasshoppers are known to appear regularly or occasionally. In our study, sampling locations were established at intervals of approximately 10 km. Within each of these sampling locations, individual sampling points were positioned at intervals averaging 100 m, with each point being revisited and resampled three times to ensure data reliability. To eliminate potential spatial autocorrelation, the grassland data were spatially rarefied with a radius of one kilometer, and observational grasshopper occurrence data were randomly assigned to the appropriate vegetation regions. Additionally, land cover data from 2020, which provided accurate geographic information about grasslands, were obtained from the Resource and Environment Science and Data Centre (https://www.resdc.cn/, retrieved on 5 March 2024).

2.3. Data Analysis

Figure 2 depicts the analysis process. First, pertinent habitat factors were carefully chosen from a variety of sources and attained through field surveys conducted within the specified research region. After that, a Python-based batch processing algorithm was employed in ArcGIS 10.8 to preprocess the data, ensuring a consistent data coordinate system and spatial resolution. Next, the factors employed in this investigation were either acquired at a resolution of 1 km or rescaled to 1 km via the nearest-neighbor approach. Then, applying Pearson correlation coefficients, we found 26 major influencing components related to grasshopper dispersal. Subsequently, we obtained habitat suitability through the MaxEnt and FR approaches, and we used ROC curves and the AUC measure to evaluate the modeling results. Then, a classification was performed to determine suitable habitat areas. Finally, an extensive analysis was performed to identify the main factors used in the dispersal of grasshoppers.

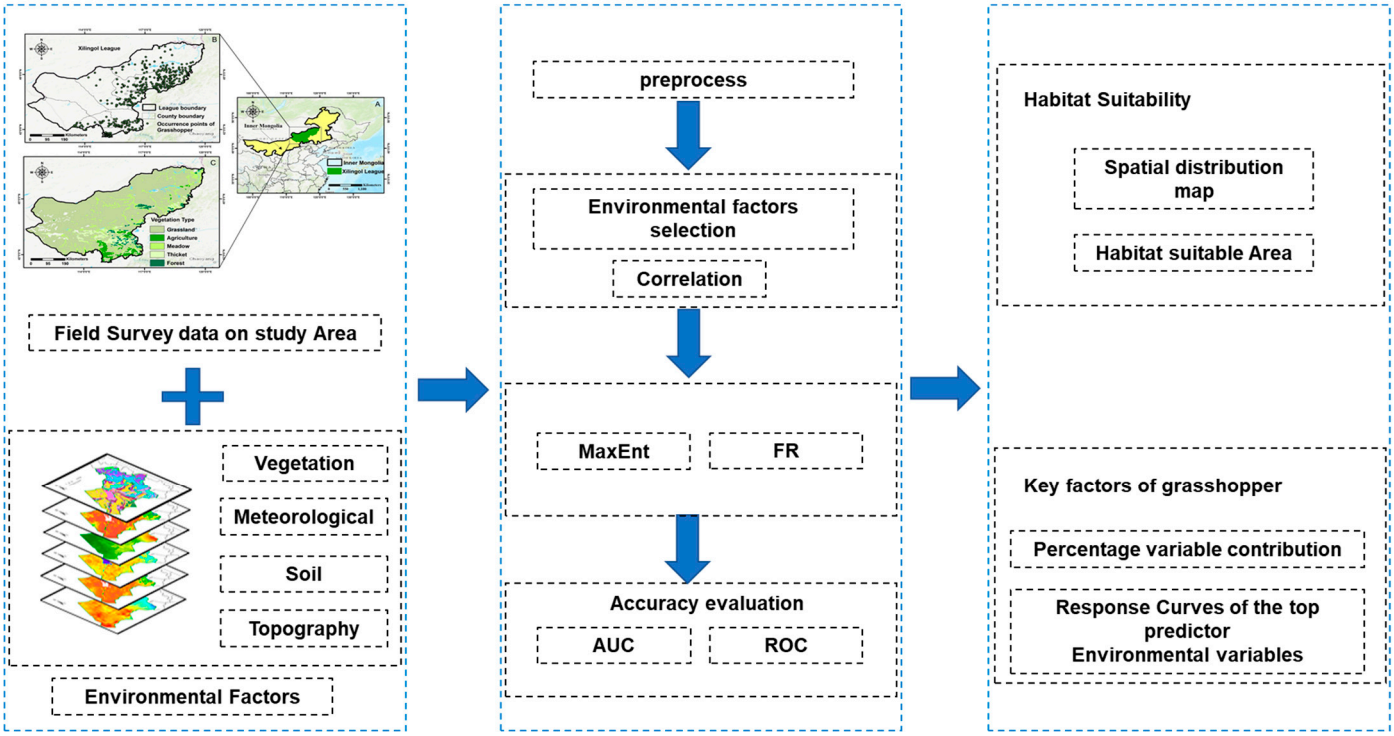


Figure 2. Analysis process for the assessment of habitat suitability for *Oedaleus decorus asiaticus* using MaxEnt and frequency ratio approaches in Xilingol League, China. First blue box is the combination of field survey data and environmental factors, second box represent the modelling process and accuracy evaluation, third box shows the final results, whereas the blue arrows represent the work flow of analysis.

2.3.1. Determination of Grasshopper Development Stage

Xilingol is home to several dozen species, with the most prevalent being *Oedaleus decorus asiaticus* (Bey-Bienko) and *Dasyhippus barbipes* (Fischer von Waldheim). We classify *Dasyhippus barbipes* as an early-hatching species that leads to minimal damage to grassland ecosystems. We classify *Oedaleus decorus asiaticus* as an early-intermediate hatching species that undergoes its growth phase during the period of pasture thriving [11]. Moreover, it possesses the traits of aggregation, movement, and robust reproductive capability, resulting in significant devastation to grassland ecosystems. Furthermore, most of the data are based on *Oedaleus decorus asiaticus*, as our study was conducted during this species' growth season. This research focuses on *Oedaleus decorus asiaticus*.

Grasshoppers go through three developmental stages: egg, nymph, and adult phases. Grasshoppers hatch and enter the first instar stage when the temperature reaches their developmental initiation temperature. Next, in five or six instars, the grasshoppers will undergo a period of experience that lasts one to two months. This stage is known as the nymph stage, and it lasts from the first instar all the way up to the fifth or sixth instar. Following completion of the nymph stage, they experience eclosion and metamorphose into maturity. After finding a partner, an adult grasshopper selects an appropriate place and conditions to lay its eggs. Most of the time, grasshoppers prefer days that are sunny and have warm ambient conditions. The eggs overwinter in soil after spawning. The egg stage is the time frame from spawning to hatching the following year. Based on prior research, the development of grasshoppers can be roughly divided into three stages: the egg stage (mid-to-late August of the previous year until mid-to-late May of the current year), the nymph stage (mid-to-late May until early July), and the adult stage (early July to mid-to-late August) [11].

2.3.2. Selection of Environmental Factors

The correlation between environmental factors within the same class may diminish the model's outcome [60]. We used the correlation visualization tool in R to examine the relationships between all of the factors. To prevent a high degree of collinearity among variables, only variables with Pearson correlation coefficients below 0.8 were chosen [61]. The factors that were ultimately chosen, as shown in Table 1, were as follows: ELST, NLST, ESH, Elevation, ASH, EP, NP, AP, NAB, VT, ESM, NSM, Aspect, ASM, ESI, NSI, ASI, SSAND, Slope, SOC, SpH, SSILT, SBD, SN, SCC, and ST.

Table 1. The environmental factors. Altogether, there are **26** factors.

Category	Factors	Development Stage	Data Source	Spatial Resolution	Temporal Resolution
Meteorology	Mean LST	Egg Nymph	MOD11A1	1 km	1 day
	Mean Specific Humidity	Egg Adult	FLDAS	11,132 m	1 day
	Mean Precipitation	Egg Nymph Adult	GPM	11,132 m	Monthly
Vegetation	Above-ground Biomass	Nymph	MOD13A2	1 km	16 days
	Vegetation Type	Static Factor	Chinese Academy of Sciences	1 km	
Soil	Soil Moisture	Egg Nymph Adult	FLDAS	11,132 m	Monthly
	Soil Salinity index	Egg Nymph Adult	MOD09A1	1 km	8 days
	Soil Sand	Static Factor	Soil Grids	250 m	
	Soil Organic Carbon	Static Factor	Soil Grids	250 m	
	Soil Ph	Static Factor	Soil Grids	250 m	
	Soil Silt	Static Factor	Soil Grids	250 m	
	Soil Bulk Density	Static Factor			
	Soil Nitrogen	Static Factor	Soil Grids	250 m	
	Soil Clay Content	Static Factor	Soil Grids	250 m	

	Soil Type	Static Factor	Chinese Academy of Sciences	1 km
Topographic	Elevation	Static Factor	Chinese Academy of Sciences	90 m
	Slope	Static Factor	Chinese Academy of Sciences	90 m
	Aspect	Static Factor	Chinese Academy of Sciences	90 m

2.3.3. Extraction Method of Habitat Suitability

1. MaxEnt approach

We used MaxEnt software (Version 3.4.1) in this work to extract the habitat suitability. You can access the software at https://biodiversityinformatics.amnh.org/open_source/MaxEnt/. MaxEnt is a Java-based species distribution approach that derives a species' probability distribution map from its occurrence data and environmental variables by applying the maximum entropy method. This model demonstrates high accuracy in predicting the habitat distributions of niche species and examining their correlations with environmental factors [62]. The theoretical foundation of MaxEnt is based on the principle of maximum entropy, which seeks to estimate the probability distribution of a species' occurrence by maximizing the entropy (i.e., uncertainty) under the constraints of the available environmental data. The model ensures that the distribution is as uniform as possible, given the known environmental conditions, without making additional assumptions beyond the observed data. According to [63], below is the MaxEnt approach formula:

$$P_w(y|x) = \frac{1}{Z_w(x)} exp\left(\sum_{i=1}^{n} w_i f_i\,(x,y)\right) \tag{3}$$

$$Z_w(x) = \sum_{y} exp\left(\sum_{i=1}^{n} w_i f_i\,(x,y)\right) \tag{4}$$

where x represents each input environmental variable, y denotes the location of grasshopper occurrence, $f_i(x,y)$ is the characteristics function, w_i is the weight of the characteristics function, n represents the number of datasets, and $P_w(y|x)$ is the spatial distribution of the grasshopper habitat.

We applied the bootstrapping method to our MaxEnt model with 50 replicates. In each iteration, 30% of the occurrence data was designated as the test set, while the remaining 70% constituted the training set. The model selected these spots homogeneously and randomly, which somewhat ensured spatial independence. We configured the remaining options using their default values. Model accuracy was evaluated using ROC curves and AUC values, which provide a measure of predictive performance. Additionally, we quantify the individual roles of the elements as percentages to identify the important factors affecting grasshopper presence. MaxEnt's ability to handle complex ecological interactions and produce accurate predictions with limited data makes it highly effective for this study, as demonstrated by its widespread use in species distribution modeling, invasive species management, and pest control.

2. Frequency ratio (FR) approach

The spatial relationship between the presence of grasshoppers (dependent variable) and the variables that contribute to grasshopper outbreaks (independent variables) is illustrated by the FR approach. We determined the FR value of each variable by

quantitatively assessing the relationships between the independent variables and grasshopper occurrence. When the weight of FR is greater than 1, it signifies a robust correlation, whereas a weight below 1 suggests a poor connection between the dependent and independent factors. We computed the FR value using the following formula:

$$FR = \frac{\frac{GP}{P}}{\frac{FA}{A}} \quad (5)$$

where in Equation (5), FA represents the factor class area, GP represents the grasshopper point in the factor class, A represents the overall area, and P represents the total grasshopper points. Subsequently, the RF value was computed to standardize the FR value within the probability interval of (0, 1) using Equation (6):

$$RF = \frac{FR\ of\ factor\ class}{\sum FR\ of\ factor\ classes} \quad (6)$$

Then, using the provided Equation (7), we calculated the prediction rate (PR) to assess the correlations between factors that cause grasshopper infestations and the training dataset:

$$PR = \frac{(RF_{max} - RF_{min})}{(RF_{max} - RF_{min})_{Min}} \quad (7)$$

The habitat suitability map for grasshoppers was created by categorizing and computing the grasshopper habitat suitability index (GHSI). The GHSI assesses the area's suitability for grasshopper occurrence. Regions with higher GHSI values suggest a larger likelihood of grasshopper presence, whereas regions with lower GHSI values indicate a lower likelihood of grasshopper presence. Equations (6) and (7) determined the RF and PR values, which we used to compute the GHSI. Equation (8) depicts the GHSI calculation:

$$GHSI = \sum_{i=1}^{26} PR_i \times RF_i \quad (8)$$

In the above equation, 26 denotes the number of factors contributing to grasshopper infestations. We classified the resulting grasshopper habitat suitability map into three categories [64]. The total number of grasshopper data points was randomly allocated, with 70% designated for the FR approach as training points and 30% reserved for testing and validation purposes. We used FR values (Table 2) to determine the bivariate correlation between habitat suitability parameters and actual grasshopper infestation zones.

The FR value for each factor determines the degree of suitability of the grasshopper habitat. Soil salinity index in the egg stage (ESI) was classified into five classes. The significance level of FR exhibited an inverse correlation with ESI. For example, the first salinity class (class 1) had a greater FR score (2.55). Conversely, when the soil salinity index rose, the FR score steadily dropped until the 5th soil salinity index class exhibited a zero FR score. Additionally, five classes of EP had a positive correlation with FR. The value started at 0 for the first class, indicating a lower EP value, then ascended to a maximum of 3.59, reflecting a greater EP value. The remaining factors were examined similarly, as outlined in Table 2.

Table 2. Details of the habitat suitability factors and their FR values.

Factor	Class	Points	% Points	Class Area	% Class Area	FR	RF
ESI	1	62,000,000	80.52	64,116	31.60	2.55	0.75
	2	12,000,000	15.58	49,731	24.51	0.64	0.19
	3	3,000,000	3.90	39,270	19.36	0.20	0.06
	4	0	0.00	35,977	17.73	0.00	0.00

	5	0	0.00	13,773	6.79	0.00	0.00
EP	1	0	0.00	37,060	18.27	0.00	0.00
	2	1,000,000	1.30	36,785	18.13	0.07	0.01
	3	3,000,000	3.90	43,345	21.37	0.18	0.03
	4	28,000,000	36.36	52,691	25.97	1.40	0.27
	5	45,000,000	58.44	32,986	16.26	3.59	0.68
Slope	1	20,000,000	25.97	87,820	43.85	0.59	0.04
	2	24,000,000	31.17	68,383	34.14	0.91	0.07
	3	28,000,000	36.36	34,314	17.13	2.12	0.16
	4	3,000,000	3.90	9201	4.59	0.85	0.06
	5	2,000,000	2.60	574	0.29	9.06	0.67
ASM	1	0	0.00	47,304	23.38	0.00	0.00
	2	12,000,000	15.58	70,317	34.75	0.45	0.08
	3	42,000,000	54.55	60,071	29.69	1.84	0.31
	4	23,000,000	29.87	16,735	8.27	3.61	0.61
	5	0	0.00	7915	3.91	0.00	0.00
NSI	1	35,000,000	45.45	34,491	17.00	2.67	0.57
	2	37,000,000	48.05	57,516	28.35	1.69	0.36
	3	4,000,000	5.19	45,617	22.49	0.23	0.05
	4	1,000,000	1.30	43,141	21.27	0.06	0.01
	5	0	0.00	22,102	10.89	0.00	0.00
ESM	1	0	0.00	30,855	15.25	0.00	0.00
	2	5,000,000	6.49	57,184	28.26	0.23	0.05
	3	30,000,000	38.96	58,428	28.88	1.35	0.29
	4	39,000,000	50.65	38,746	19.15	2.65	0.56
	5	3,000,000	3.90	17,129	8.47	0.46	0.10
ELST	1	37,000,000	48.05	30,451	15.01	3.20	0.58
	2	15,000,000	19.48	44,908	22.14	0.88	0.16
	3	10,000,000	12.99	35,115	17.31	0.51	0.09
	4	13,000,000	16.88	51,435	25.35	0.84	0.15
	5	2,000,000	2.60	40,958	20.19	0.13	0.02
AP	1	0	0.00	47,891	23.61	0.00	0.00
	2	2,000,000	2.60	56,521	27.86	0.09	0.02
	3	9,000,000	11.69	33,344	16.44	0.71	0.12
	4	45,000,000	58.44	38,543	19.00	3.08	0.52
	5	21,000,000	27.27	26,568	13.10	2.08	0.35
SBD	1	0	0.00	1241	0.61	0.00	0.00
	2	7,000,000	9.09	10,980	5.41	1.68	0.31
	3	44,000,000	57.14	44,682	22.03	2.59	0.48
	4	24,000,000	31.17	60,234	29.69	1.05	0.19
	5	2,000,000	2.60	85,723	42.26	0.06	0.01
ASI	1	30,000,000	38.96	37,877	18.67	2.09	0.44
	2	37,000,000	48.05	47,880	23.60	2.04	0.43
	3	9,000,000	11.69	43,911	21.65	0.54	0.11
	4	1,000,000	1.30	42,279	20.84	0.06	0.01
	5	0	0.00	30,920	15.24	0.00	0.00
Elevation	1	34,000,000	44.16	40,635	20.03	2.20	0.46
	2	28,000,000	36.36	58,161	28.67	1.27	0.26
	3	7,000,000	9.09	47,141	23.24	0.39	0.08
	4	2,000,000	2.60	36,669	18.08	0.14	0.03
	5	6,000,000	7.79	20,261	9.99	0.78	0.16
ASH	1	3,000,000	3.90	45,378	22.37	0.17	0.03

	2	3,000,000	3.90	40,005	19.72	0.20	0.03
	3	10,000,000	12.99	51,111	25.19	0.52	0.09
	4	38,000,000	49.35	42,492	20.95	2.36	0.41
	5	23,000,000	29.87	23,881	11.77	2.54	0.44
SSAND	1	0	0.00	1240	0.61	0.00	0.00
	2	3,000,000	3.90	32,407	15.98	0.24	0.06
	3	22,000,000	28.57	66,413	32.74	0.87	0.22
	4	32,000,000	41.56	69,927	34.47	1.21	0.31
	5	20,000,000	25.97	32,873	16.20	1.60	0.41
SCC	1	0	0.00	1240	0.61	0.00	0.00
	2	37,000,000	48.05	62,791	30.95	1.55	0.41
	3	24,000,000	31.17	76,572	37.75	0.83	0.22
	4	10,000,000	12.99	42,880	21.14	0.61	0.16
	5	6,000,000	7.79	19,377	9.55	0.82	0.21
NP	1	0	0.00	69,863	34.44	0.00	0.00
	2	22,000,000	28.57	69,085	34.05	0.84	0.13
	3	38,000,000	49.35	37,945	18.70	2.64	0.40
	4	15,000,000	19.48	15,587	7.68	2.54	0.39
	5	2,000,000	2.60	10,387	5.12	0.51	0.08
NSM	1	0	0.00	41,029	19.68	0.00	0.00
	2	17,000,000	22.08	63,030	30.23	0.73	0.13
	3	29,000,000	37.66	47,875	22.96	1.64	0.28
	4	15,000,000	19.48	37,859	18.16	1.07	0.19
	5	16,000,000	20.78	18,699	8.97	2.32	0.40
ESH	1	4,000,000	5.19	21,928	10.81	0.48	0.13
	2	14,000,000	18.18	40,834	20.13	0.90	0.24
	3	22,000,000	28.57	65,204	32.14	0.89	0.23
	4	37,000,000	48.05	64,211	31.65	1.52	0.40
	5	0	0.00	10,690	5.27	0.00	0.00
ST	1	0	0.00	22	0.01	0.00	0.00
	2	0	0.00	204	0.10	0.00	0.00
	3	2,000,000	2.70	1706	0.87	3.09	0.35
	4	13,000,000	17.57	11,203	5.74	3.06	0.34
	5	53,000,000	71.62	112,340	57.55	1.24	0.14
	6	0	0.00	27,235	13.95	0.00	0.00
	7	0	0.00	23,786	12.19	0.00	0.00
	8	0	0.00	309	0.16	0.00	0.00
	9	0	0.00	1118	0.57	0.00	0.00
	10	6,000,000	8.11	10,629	5.45	1.49	0.17
	11	0	0.00	2549	1.31	0.00	0.00
	12	0	0.00	2748	1.41	0.00	0.00
	13	0	0.00	1049	0.54	0.00	0.00
	14	0	0.00	292	0.15	0.00	0.00
SpH	1	0	0.00	1240	0.61	0.00	0.00
	2	3,000,000	3.90	6147	3.03	1.29	0.28
	3	15,000,000	19.48	25,802	12.72	1.53	0.34
	4	47,000,000	61.04	93,060	45.87	1.33	0.29
	5	12,000,000	15.58	76,611	37.77	0.41	0.09
VT	1	66,000,000	86.84	154,887	78.96	1.10	0.28
	2	4,000,000	5.26	20,207	10.30	0.51	0.13
	3	2,000,000	2.63	4297	2.19	1.20	0.31
	4	4,000,000	5.26	9790	4.99	1.05	0.27
	5	0	0.00	6967	3.55	0.00	0.00

SSILT	1	0	0.00	1241	0.61	0.00	0.00
	2	14,000,000	18.18	28,233	13.93	1.30	0.33
	3	28,000,000	36.36	64,612	31.89	1.14	0.29
	4	29,000,000	37.66	72,076	35.57	1.06	0.27
	5	6,000,000	7.79	36,445	17.99	0.43	0.11
NAB	1	9,000,000	11.69	108,993	53.73	0.22	0.03
	2	40,000,000	51.95	61,521	30.33	1.71	0.21
	3	22,000,000	28.57	21,327	10.51	2.72	0.33
	4	3,000,000	3.90	7791	3.84	1.01	0.12
	5	3,000,000	3.90	3218	1.59	2.46	0.30
NLST	1	8,000,000	10.39	10,658	5.25	1.98	0.32
	2	13,000,000	16.88	24,280	11.97	1.41	0.23
	3	26,000,000	33.77	46,658	23.00	1.47	0.24
	4	28,000,000	36.36	58,846	29.01	1.25	0.20
	5	2,000,000	2.60	62,425	30.77	0.08	0.01
SN	1	0	0.00	27,935	13.77	0.00	0.00
	2	29,000,000	37.66	71,763	35.38	1.06	0.23
	3	32,000,000	41.56	65,365	32.22	1.29	0.28
	4	13,000,000	16.88	30,436	15.00	1.13	0.25
	5	3,000,000	3.90	7361	3.63	1.07	0.24
SOC	1	3,000,000	3.90	83,425	41.12	0.09	0.01
	2	37,000,000	48.05	63,045	31.08	1.55	0.21
	3	21,000,000	27.27	35,701	17.60	1.55	0.21
	4	13,000,000	16.88	16,954	8.36	2.02	0.28
	5	3,000,000	3.90	3735	1.84	2.12	0.29
Aspect	1	14,000,000	18.18	36,358	18.15	1.00	0.20
	2	21,000,000	27.27	38,029	18.99	1.44	0.29
	3	12,000,000	15.58	36,619	18.28	0.85	0.17
	4	13,000,000	16.88	39,951	19.95	0.85	0.17
	5	17,000,000	22.08	49,335	24.63	0.90	0.18

3. Results

3.1. Habitat Suitability Results Using the MaxEnt Approach

The findings obtained using the MaxEnt approach regarding the suitability for grasshopper occurrence in the Xilingol region are depicted in Figure 3. The appropriateness for grasshopper occurrence is categorized into three levels: less suitable (0–0.5), moderately suitable (0.5–0.7), and most suitable (0.7–1) [58]. Within the Xilingol region, 1% of the research area is classified as most suitable, 5% as moderately suitable, and the remaining 94% as less suitable for grasshopper occurrence. Our MaxEnt analysis revealed that the most suitable and moderately suitable habitats for grasshoppers are predominantly concentrated in the southern and eastern parts of Xilingol League, including areas such as West Ujumqin, East Ujumqin, Xilinhot, Duolun, Taipusi, Xianghuang, Zhenglan, and Zheng Xiangbai. The distribution pattern indicates that these regions provide environmental conditions that are particularly favorable for the presence and activity of grasshoppers. By contrast, the less suitable habitats, as identified by MaxEnt, are primarily located in the northern and western parts of Xilingol League, where conditions may be less conducive to the survival and breeding of grasshoppers.

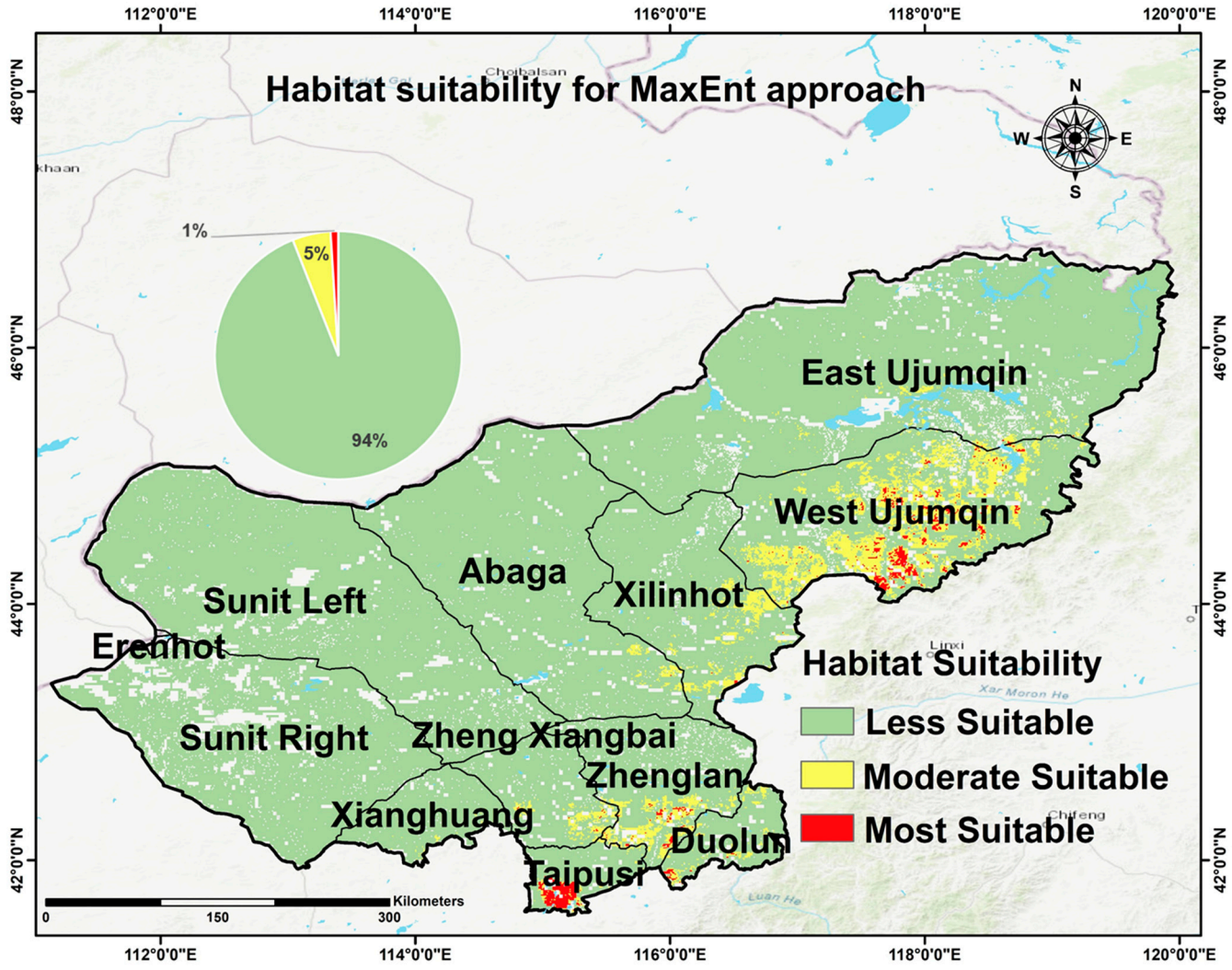


Figure 3. Habitat suitability for *O. d. asiaticus* occurrence using the MaxEnt approach.

3.2. Habitat Suitability Results Using the FR Approach

Figure 4 presents the findings obtained using the FR approach to grasshopper occurrence suitability in Xilingol. We divided the map into three distinct categories: less suitable (108–550), moderately suitable (550–750), and most suitable (750–1100). Additionally, our findings show that 2% of the study area in Xilingol is most suitable for grasshopper occurrence, 6% is moderately suitable, and the remaining 92% is less suitable. The FR approach yielded a similar yet distinct pattern in the distribution of suitable habitats. The most suitable and moderately suitable areas, as determined by the FR approach, are mainly located in the northern, southern, and eastern parts of Xilingol League, with specific concentrations in West Ujumqin, East Ujumqin, Duolun, Taipusi, and Zhenglan. This indicates that the FR approach also recognizes the importance of these areas for grasshopper habitat suitability, with a slightly different emphasis on the northern regions compared to MaxEnt. According to the FR approach, the less suitable habitats are primarily distributed in the western parts of Xilingol League, aligning with the MaxEnt findings but with a different distribution. In summary, both the MaxEnt and FR approaches consistently identified the southern and eastern parts of Xilingol League as critical for grasshopper habitat suitability, although there were subtle variations in the specific regions classified as most suitable.

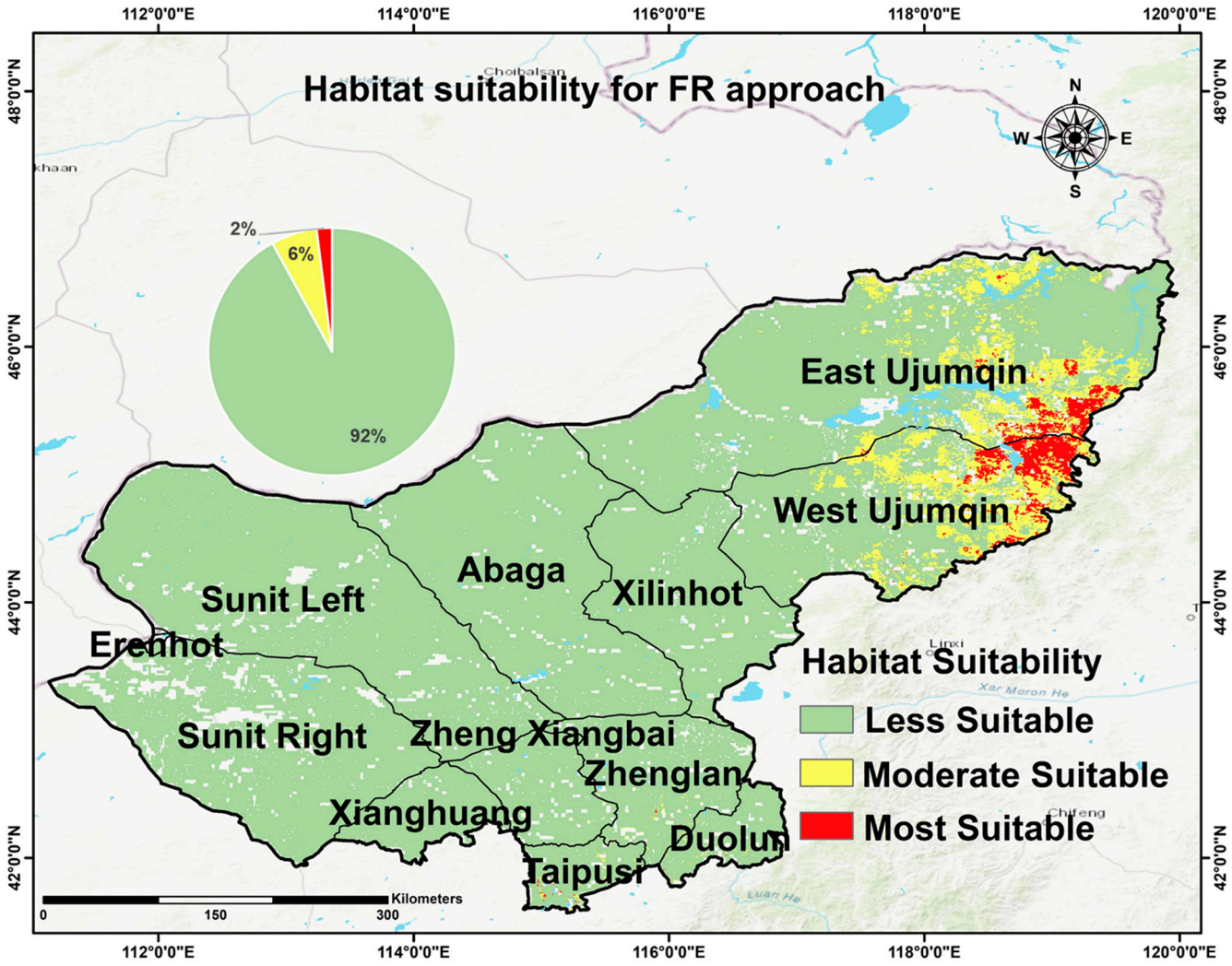


Figure 4. Habitat suitability for *O. d. asiaticus* occurrence using the FR approach.

3.3. Accuracy Evaluation

The received operating characteristic (ROC) curve was utilized to assess the accuracy of the grasshopper occurrence model in the study area. We employed a 70% training dataset to evaluate the success rate, as depicted in Figure 5a, and a 30% testing dataset to validate the model's performance, as shown in Figure 5b. As shown in Figure 5, the MaxEnt approach achieved a 92.4% success rate with the training dataset and a 93.9% validation rate with the testing dataset. Similarly, the frequency ratio (FR) approach yielded an 86.9% success rate with the training dataset and an 86.7% validation rate with the testing dataset. Nonetheless, both approaches had satisfactory success rates and validation rates.

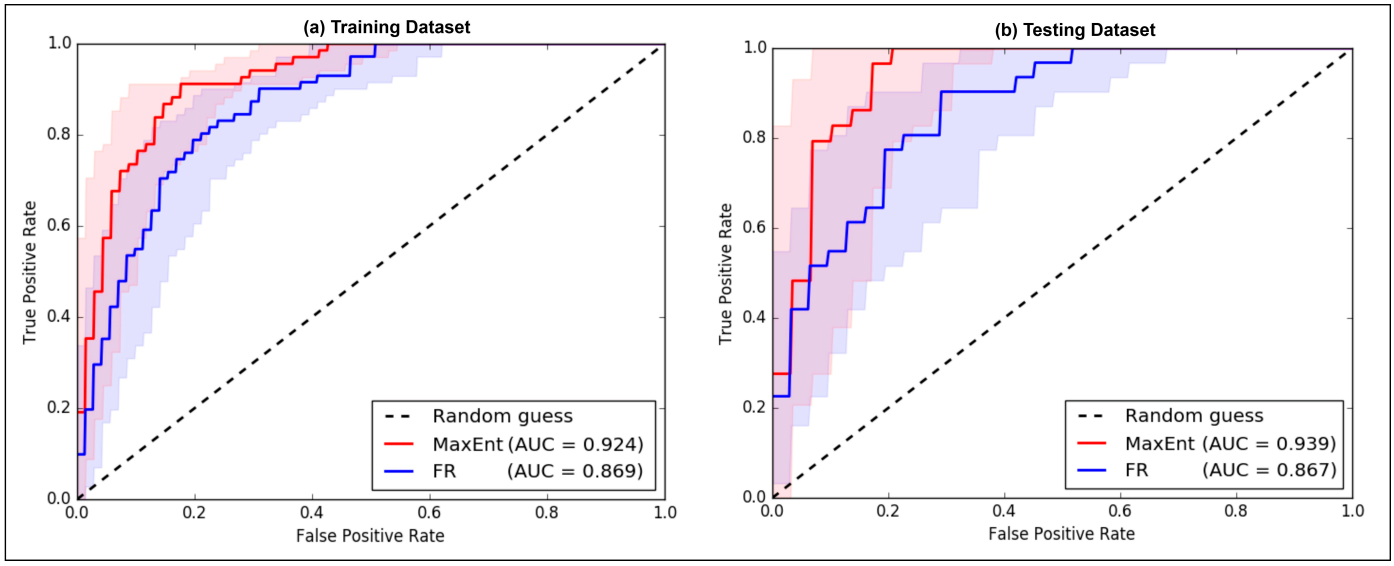


Figure 5. (**a**) Success curves of the approaches using the training dataset; (**b**) Validation curves using the testing dataset. The red color in the pictures represents the MaxEnt model, while the blue color represents the FR model.

3.4. Contribution of Habitat Factors Affecting O. d. asiaticus Distribution

To mitigate significant collinearity among the variables, we maintained those with Pearson's correlation values less than 0.8 (Figure 6). Thus, 26 factors were chosen, including **ASI, SBD, ESI, ELST, NSI, SSILT, SCC, SpH, NLST, Elevation, NAB, SOC, SN, ST, Aspect, Slope, VT, SSAND, EP, ASM, NSM, AP, ESM, NP, ASH, and ESH**. The factors encompassed four categories: vegetation, soil, topography, and meteorology. In this study, the most important variables were those for which the combined values were more than 80% [65]. The designated vital factors for the year 2022 are illustrated in Table 3.

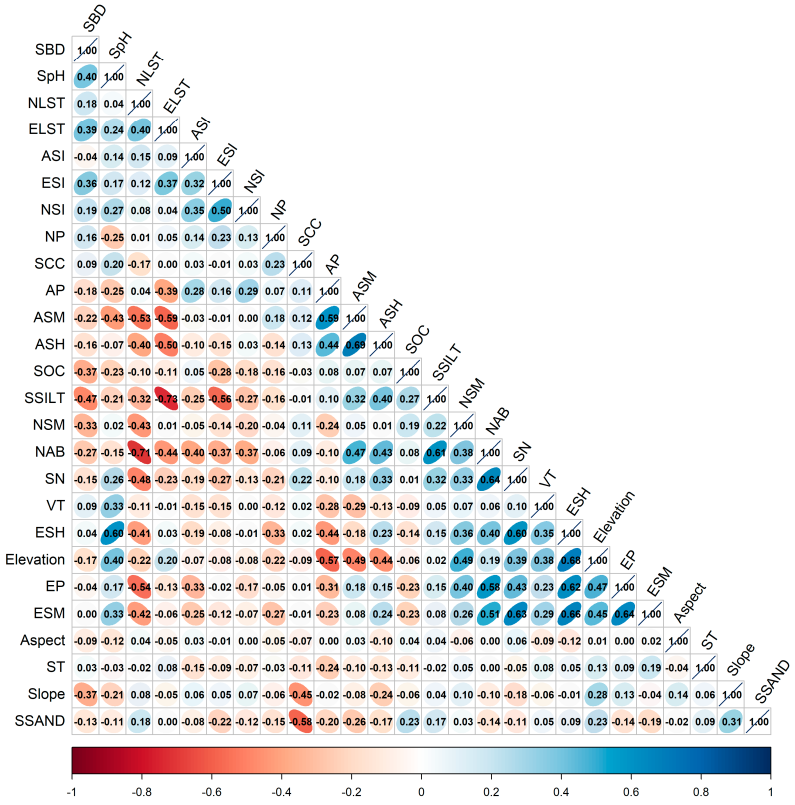


Figure 6. The correlations of each habitat factor. Red indicates a negative correlation, and Blue indicates a positive correlation, while White or lighter colors indicate a lack of correlation or a very weak correlation

Table 3. Relative contributions of the environmental variables to grasshopper occurrence.

Environmental Factor	Percentage Contribution
ASH	23.8%
VT	19.7%
NAB	8.8%
SSAND	8.4%
EP	5.7%
NP	4.4%
SBD	3.7%
Elevation	3%
ST	2.9%
Total	80.4%

The mean specific humidity during the adult stage (**ASH**), vegetation type (**VT**), above-ground biomass during the nymph stage (**NAB**), soil sand content (**SSAND**), mean precipitation during the egg stage (**EP**), mean precipitation during the nymph stage (**NP**), soil bulk density (**SBD**), **Elevation**, and soil type (**ST**) possessed the highest predictive power for modeling grasshopper occurrence in Xilingol, as indicated in Table 3. The contributions were 23.8%, 19.7%, 8.8%, 8.4%, 5.7%, 4.4%,3.7%, 3%, and 2.9%, respectively.

The FR approach analyzed real grasshopper points and habitat factors in a bivariate manner. Table 4 indicates that the soil salinity index during the egg stage (**ESI**), which has the highest PR value (8.71), was the primary factor influencing habitat suitability. The PR values of 7.93 for mean precipitation during the egg stage (**EP**) and 7.24 for the **slope** ranked them next to one another, respectively. Conversely, Aspect was regarded as the least significant habitat suitability feature, with a PR value of 1.

Table 4. PR values of grasshopper occurrence factors and their contributions to habitat suitability.

Factor	Min RF	Max RF	Max–Min RF	(Max–Min) Min RF	PR Value
ESI	0.00	0.75	0.75	0.09	8.71
EP	0.00	0.68	0.68	0.09	7.93
Slope	0.04	0.67	0.63	0.09	7.24
ASM	0.00	0.61	0.61	0.09	7.09
NSI	0.00	0.57	0.57	0.09	6.64
ESM	0.00	0.56	0.56	0.09	6.54
ELST	0.02	0.58	0.55	0.09	6.40
AP	0.00	0.52	0.52	0.09	5.97
SBD	0.00	0.48	0.48	0.09	5.58
ASI	0.00	0.44	0.44	0.09	5.11
Elevation	0.03	0.46	0.43	0.09	4.98
ASH	0.03	0.44	0.41	0.09	4.73
SSAND	0.00	0.41	0.41	0.09	4.73
SCC	0.00	0.41	0.41	0.09	4.72
NP	0.00	0.40	0.40	0.09	4.68
NSM	0.00	0.40	0.40	0.09	4.66
ESH	0.00	0.40	0.40	0.09	4.64
ST	0.00	0.35	0.35	0.09	4.03

SpH	0.00	0.34	0.34	0.09	3.89
SSILT	0.00	0.33	0.33	0.09	3.84
VT	0.00	0.00	0.00	0.09	3.59
NAB	0.03	0.33	0.31	0.09	3.56
NLST	0.01	0.32	0.31	0.09	3.54
SN	0.00	0.28	0.28	0.09	3.28
SOC	0.01	0.29	0.28	0.09	3.19
Aspect	0.20	0.29	0.09	0.09	1.00

3.5. The Influence of Principal Contributing Factors on Grasshopper Presence in Xilingol League

Figure 7 presents the response curves delineating the correlations between the habitat suitability for *O. d. asiaticus* and major environmental drivers. The suitability for *O. d. asiaticus* is at its highest when the mean specific humidity during the adult stages is within the range of 0.0080 to 0.0095 (mass fraction), peaking at 0.0092 (mass fraction). During the nymph stage, the suitability for *O. d. asiaticus* is high when the above-ground biomass is between 100 kg/hm^3 and 180 kg/hm^3, and it reaches its peak at 140 kg/hm^3. Regarding soil sand content, the suitability increases rapidly when it is less than 500 g/kg and reaches its peak at 600 g/kg. During the egg phase, *O. d. asiaticus* exhibits a positive correlation with precipitation levels, which is particularly evident when the monthly precipitation is less than 0.017 mm. Moreover, the most favorable conditions for *O. d. asiaticus* are observed within the precipitation range of 0.035 to 0.040 mm. The suitability for *O. d. asiaticus* is enhanced when the average nymph stage precipitation is less than 0.15 mm and decreases when it exceeds 0.20 mm. The suitability reaches its highest value when the soil bulk density is 1.35 g/cm^3. The suitability is high when the elevation is between 800 and 850 m or between 1250 and 1450 m, and it reaches its peak at 1400 m.

The Northwest *Stipa* grassland, *Leymus chinensis*, tiger hazelnut bush, and birch forest were categorized as highly suitable habitats, with respective suitability indices of 0.99, 0.97, 0.96, and 0.94, as presented in Table 5**.** Furthermore, chestnut, meadow, tidal, and gray forest soil also demonstrated suitability, with indices of 0.68, 0.62, 0.61, and 0.58, respectively, as detailed in Table 5.

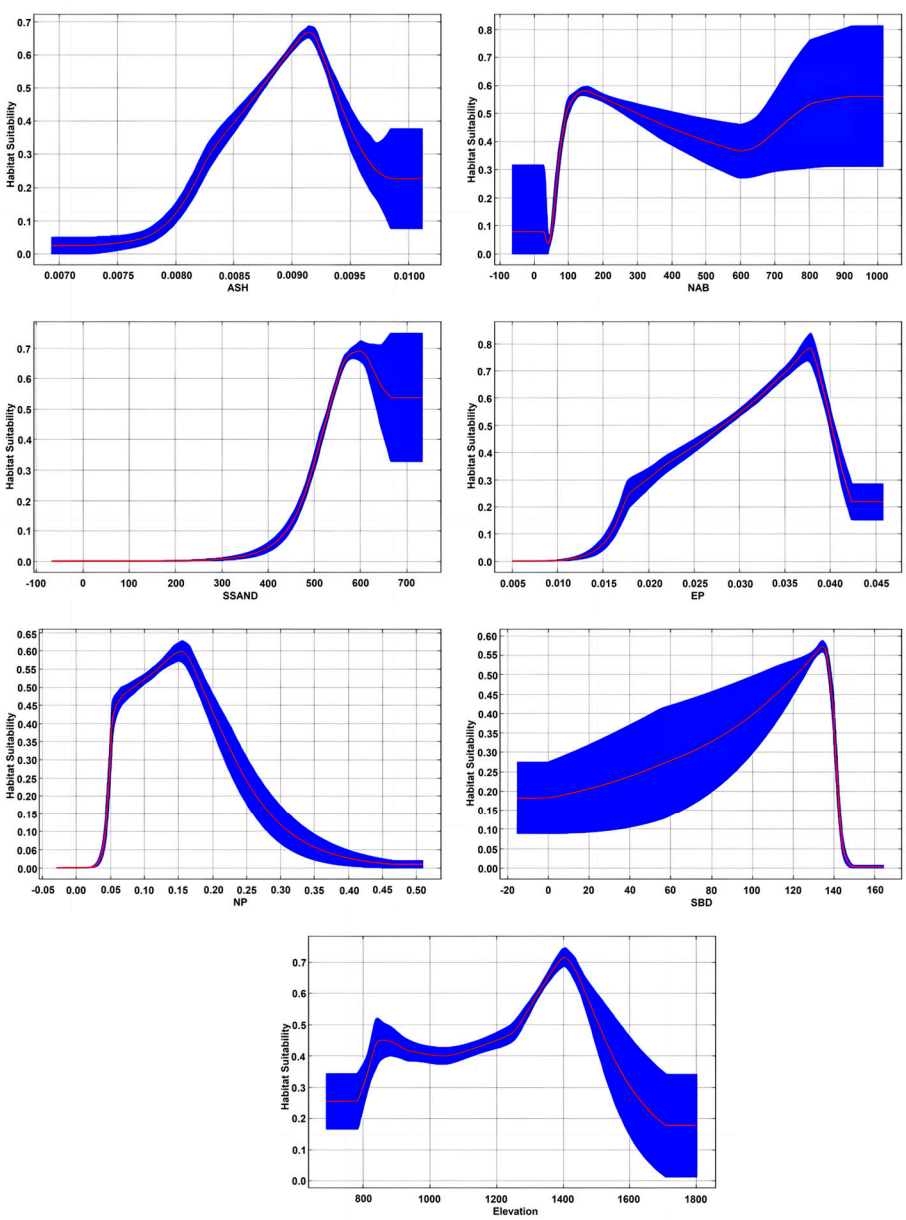


Figure 7. Response curves for key environmental variables affecting grasshopper occurrence using the MaxEnt approach. The ordinate axis shows suitability, and the abscissa axis shows a range of factors. ASH: mean specific humidity in the adult stage; NAB: above-ground biomass in the nymph stage; SSAND: soil sand content; EP: mean precipitation in the egg stage; NP: mean precipitation in the nymph stage; SBD: soil bulk density; Elevation.

Table 5. Habitat factors and their suitability. VT: vegetation type; ST: soil type.

Habitat Factor	Type Name	Suitability
VT	Northwest stipa grassland	0.99
VT	Leymus chinensis tufted grassland	0.97
VT	Tiger hazelnut bush	0.96
VT	Birch forest	0.94
ST	Chestnut soil	0.68
ST	Meadow soil	0.62
ST	Tidal soil	0.61
ST	Gray forest	0.58

4. Discussion

Grasshopper infestations constitute a significant crisis in China, annually threatening agriculture and livestock in northern regions. Nonetheless, the extensive grassland regions in northern China exhibit spatial variabilities in climatic, topographical, soil type, and grassland type characteristics. Consequently, conducting a comprehensive survey of possible grasshopper outbreak regions within a limited timeframe is challenging. The advancement of satellite remote sensing technologies has enabled rapid and efficient monitoring and forecasting of possible grasshopper outbreak regions [66]. This study delineated three developmental stages of grasshoppers based on predominant species, field survey data, and prior research. Consequently, we meticulously identified and refined four categories of environmental parameters, including soil, topographical, meteorological, and vegetation, ultimately leading to the selection of 26 factors. We accurately extracted and categorized habitat suitability into three levels using the MaxEnt and FR approaches, integrated with remote sensing data. This classification revealed the likelihood of grasshopper invasion within the research area. Finally, we pinpointed the main factors influencing the presence of grasshoppers in the study region. Compared to prior research utilizing the MaxEnt approach to identify GPH in Xilingol League [1], our work demonstrates enhanced accuracy. This enhancement mostly results from incorporating additional environmental elements contributing to grasshopper infestation.

The habitat suitability for *O. d. asiaticus* increased with average nymph stage precipitation below 0.15 mm and decreased when precipitation levels exceeded 0.20 mm. The hatching rate of *O. d. asiaticus* decreased when exposed to extended periods of immersion in warm, moist soil, supporting findings from prior research [67]. As a result, precipitation had a greater influence on the distribution of *O. d. asiaticus* than other climatic parameters. Consistent with our findings, a prior investigation reported that *O. d. asiaticus* achieves maximum habitat suitability under conditions where the above-ground biomass during the nymph stage is 140 kg/hm^3 and the elevation stands at 1400 m [58]. Subsequent analysis demonstrated that vegetation type, soil sand content, soil bulk density, and soil type significantly affected the tracking and prediction of *O. d. asiaticus* dispersion. Rainfall directly affects the ability of grasshoppers to survive and reproduce. Conversely, the type of plant indirectly shows where food and shelter are available. Due diligence in handling resolution is required to avoid any information loss, as these variables are essential to the framework. Our comprehensive assessment of habitat suitability for *O. d. asiaticus* in Xilingol League offers valuable insights for grasshopper management. By identifying the most suitable areas, we can guide targeted monitoring and early detection efforts, which are crucial for effective prevention strategies. This approach allows for more efficient chemical treatment, reducing chemical usage while maximizing impact. Identifying key environmental elements affecting grasshopper prevalence enables proactive management, potentially preventing outbreaks.

Using high-resolution remote sensing data in our study significantly enhanced the precision of habitat suitability predictions, and leveraging even higher-resolution data in the future could provide a more nuanced understanding of local habitat conditions, enriching spatial analysis and predictions. While our study is based on data collected over a specific period, it offers a solid foundation for understanding grasshopper population dynamics and environmental changes. Extending the temporal scope of our research could capture seasonal variations and long-term trends, leading to a richer understanding of the factors influencing grasshopper populations and their habitats. Although incorporating additional local-scale habitat characteristics could further enhance our models, such data are not always available or comprehensive. Our application of the MaxEnt and FR methods provided valuable insights into grasshopper distribution, but these approaches have limitations, including reliance on presence-only data and potential oversimplification of

ecological complexities. While practical, the classification-based quantification of habitat suitability may lead to inconsistencies in spatial analysis compared to gradient-based methods. Future research should explore gradient maps for a more nuanced spatial representation and consider integrating absence data or hybrid modeling approaches to improve prediction robustness. Despite these limitations, our findings remain actionable for conservation planning. Refining these models and incorporating advanced techniques will be essential to advancing ecological modeling and supporting more effective biodiversity conservation efforts.

5. Conclusions

This research used a combined methodology, analyzing soil, vegetation, meteorology, and terrain while including the occurrence tendencies of grasshoppers and their biological traits. The FR and MaxEnt approaches were used to delineate the habitat suitability for grasshoppers in Xilingol League. Initially, the relationships between the four environmental variables and the developmental behaviors of grasshoppers led to the identification of 26 factors. Subsequent MaxEnt and FR analyses revealed that most areas were categorized as less suitable, with the MaxEnt approach demonstrating high accuracy and confirming the absence of spatial autocorrelation issues. The research further discovered that the mean specific humidity during the adult stage (ASH), vegetation type (VT), above-ground biomass during the nymph stage (NAB), soil sand content (SSAND), mean precipitation during the egg stage (EP), mean precipitation during the nymph stage (NP), soil bulk density (SBD), elevation, and soil type (ST) are the key drivers of habitat suitability in Xilingol league. The habitat suitability was categorized into three distinct classes, with our analysis revealing that the most suitable and moderately suitable habitats for *O. d. asiaticus* are predominantly located in the southern and eastern parts of the Xilingol League, particularly in West Ujumqin, East Ujumqin, Xilinhot, Zhenglan, Zheng Xiangbai, Duolun, and Taipusi. This study offers methodological assistance for the early detection, effective prevention, and management of grasshopper infestations. The next investigation should focus on enhancing the use of high-resolution data, locally based environmental variables, and advanced analytical methodologies such as random forest, convolutional neural networks, and artificial neural networks to improve the efficiency, precision, and dependability of model outputs in addressing grasshopper-related challenges.

Author Contributions: Conceptualization, R.A., W.H., and Y.D.; methodology, R.A., J.G., W.H., and Z.U.R.; software, R.A.; validation, R.A.; formal analysis, R.A.; investigation, R.A.; resources, B.D., Y.Z., and F.Y.; data curation, W.H. and X.Z.; writing—original draft preparation, R.A.; writing—review and editing, R.A., W.H., and J.G.; visualization, R.A. and Z.D.; supervision, W.H. and Y.D.; project administration, W.H.; funding acquisition, W.H. All authors have read and agreed to the published version of the manuscript.

Funding: This work was supported by National Natural Science Foundation of China (42471369), The Project of Northern Agriculture and Livestock Husbandry Technical Innovation Center, Chinese Academy of Agricultural Sciences (BFGJ2022002), and Fengyun Application Pioneering Project (FY-APP-2022.0306).

Data Availability Statement: The authors do not have permission to share data.

Conflicts of Interest: The authors declare no conflicts of interest.

Abbreviations

The following abbreviations are used in this manuscript:

ASI	Soil salinity index in the adult stage
SBD	Soil bulk density
ESI	Soil salinity index in the egg stage
ELST	Mean land surface temperature in the egg stage
NSI	Soil salinity index in the nymph stage
SSILT	Soil silt content
SCC	Soil clay content
SpH	Soil pH
NLST	Mean land surface temperature in the nymph stage
NAB	Above-ground biomass in the nymph stage
SOC	Soil organic carbon
SN	Soil nitrogen content
ST	Soil type
VT	Vegetation type
SSAND	Soil sand content
EP	Mean precipitation in the egg stage
ASM	Soil moisture in the adult stage
NSM	Soil moisture in the nymph stage
AP	Mean precipitation in the adult stage
ESM	Soil moisture in the egg stage
NP	Mean precipitation in the nymph stage
ASH	Mean specific humidity in the adult stage
ESH	Mean specific humidity in the egg stage
GIS	Geographic information system

References

1. Sun, Z.; Ye, H.; Huang, W.; Qimuge, E.; Bai, H.; Nie, C.; Lu, L.; Qian, B.; Wu, B. Assessment on Potential Suitable Habitats of the Grasshopper Oedaleus Decorus Asiaticus in North China Based on MaxEnt Modeling and Remote Sensing Data. *Insects* **2023**, *14*, 138. https://doi.org/10.3390/insects14020138.
2. Lucas, J.M.; Jonas, J.; Laws, A.N.; Branson, D.H.; Pennings, S.C.; Prather, C.M.; Strickland, M.S. Functional and Taxonomic Diversity of Grasshoppers Differentially Shape Above- and Below-ground Communities and Their Function. *Funct. Ecol.* **2021**, *35*, 167–180. https://doi.org/10.1111/1365-2435.13682.
3. Olfert, O.; Weiss, R.M.; Giffen, D.; Vankosky, M.A. Modeling Ecological Dynamics of a Major Agricultural Pest Insect (*Melanoplus sanguinipes*; Orthoptera: Acrididae): A Cohort-Based Approach Incorporating the Effects of Weather on Grasshopper Development and Abundance. *J. Econ. Entomol.* **2021**, *114*, 122–130. https://doi.org/10.1093/jee/toaa254.
4. Shen, J.; Zhang, N.; Gexigeduren; He, B.; Liu, C.-Y.; Li, Y.; Zhang, H.-Y.; Chen, X.-Y.; Lin, H. Construction of a GeogDetector-Based Model System to Indicate the Potential Occurrence of Grasshoppers in Inner Mongolia Steppe Habitats. *Bull. Entomol. Res.* **2015**, *105*, 335–346. https://doi.org/10.1017/S0007485315000152.
5. Cease, A.J.; Elser, J.J.; Ford, C.F.; Hao, S.; Kang, L.; Harrison, J.F. Heavy Livestock Grazing Promotes Locust Outbreaks by Lowering Plant Nitrogen Content. *Science* **2012**, *335*, 467–469. https://doi.org/10.1126/science.1214433.
6. Du, B.; Ding, X.; Ji, C.; Lin, K.; Guo, J.; Lu, L.; Dong, Y.; Huang, W.; Wang, N. Estimating Leymus Chinensis Loss Caused by Oedaleus Decorus Asiaticus Using an Unmanned Aerial Vehicle (UAV). *Remote Sens.* **2023**, *15*, 4352. https://doi.org/10.3390/rs15174352.
7. Kang, L.; Chen, Y. Dynamics of Grasshopper Communities Under Different Grazing Intensities in Inner Mongolian Steppes. *Insect Sci.* **1995**, *2*, 265–281. https://doi.org/10.1111/j.1744-7917.1995.tb00048.x.
8. Wen, F.; Lu, L.; Nie, C.; Sun, Z.; Liu, R.; Huang, W.; Ye, H. Analysis of Spatiotemporal Variation in Habitat Suitability for Oedaleus Decorus Asiaticus Bei-Bienko on the Mongolian Plateau Using Maxent and Multi-Source Remote Sensing Data. *Insects* **2023**, *14*, 492. https://doi.org/10.3390/insects14060492.
9. Zhang, L.; Hunter, D. Management of Locusts and Grasshoppers in China. *JOR* **2017**, *26*, 155–159. https://doi.org/10.3897/jor.26.20119.

10. Brunelle, T.; Chakir, R.; Carpentier, A.; Dorin, B.; Goll, D.; Guilpart, N.; Maggi, F.; Makowski, D.; Nesme, T.; Roosen, J.; et al. Reducing Chemical Inputs in Agriculture Requires a System Change. *Commun. Earth Environ.* **2024**, *5*, 369. https://doi.org/10.1038/s43247-024-01533-1.
11. Guo, J.; Lu, L.; Dong, Y.; Huang, W.; Zhang, B.; Du, B.; Ding, C.; Ye, H.; Wang, K.; Huang, Y.; et al. Spatiotemporal Distribution and Main Influencing Factors of Grasshopper Potential Habitats in Two Steppe Types of Inner Mongolia, China. *Remote Sens.* **2023**, *15*, 866. https://doi.org/10.3390/rs15030866.
12. Zhang, Y.; Dong, Y.; Huang, W.; Guo, J.; Wang, N.; Ding, X. Extraction and Analysis of Grasshopper Potential Habitat in Hulunbuir Based on the Maximum Entropy Model. *Remote Sens.* **2024**, *16*, 746. https://doi.org/10.3390/rs16050746.
13. Dong, Y.; Xu, F.; Liu, L.; Du, X.; Ren, B.; Guo, A.; Geng, Y.; Ruan, C.; Ye, H.; Huang, W.; et al. Automatic System for Crop Pest and Disease Dynamic Monitoring and Early Forecasting. *IEEE J. Sel. Top. Appl. Earth Obs. Remote Sens.* **2020**, *13*, 4410–4418. https://doi.org/10.1109/JSTARS.2020.3013340.
14. Sivanpillai, R.; Latchininsky, A.V. Special Section Guest Editorial: Advances in Remote Sensing Applications for Locust Habitat Monitoring and Management. *J. Appl. Remote Sens.* **2015**, *8*, 084801. https://doi.org/10.1117/1.JRS.8.084801.
15. Zhang, F.; Geng, M.; Wu, Q.; Liang, Y. Study on the Spatial-Temporal Variation in Evapotranspiration in China from 1948 to 2018. *Sci. Rep.* **2020**, *10*, 17139. https://doi.org/10.1038/s41598-020-74384-3.
16. Huang, K.H.J.; Huang, K.H.J.; Huang, K.H.J. Remote Sensing of Locust and Grasshopper Plague in China: A Review. In Proceedings of the 2016 Fifth International Conference on Agro-Geoinformatics (Agro-Geoinformatics), Tianjin, China, 18–20 July 2016; IEEE: 2016; pp. 1–6.
17. Guo, J.; Huang, W.; Dong, Y.; Lin, K.; Zhou, Y.; Wang, N.; Hua, R.; Hao, Z.; Ding, X.; Zhao, F. Spatiotemporal Monitoring of Grasshopper Habitats Using Multi-Source Data: Combined with Landscape and Spatial Heterogeneity. *Int. J. Appl. Earth Obs. Geoinf.* **2024**, *130*, 103838. https://doi.org/10.1016/j.jag.2024.103838.
18. Waldner, F.; Ebbe, M.; Cressman, K.; Defourny, P. Operational Monitoring of the Desert Locust Habitat with Earth Observation: An Assessment. *ISPRS Int. J. Geo-Inf.* **2015**, *4*, 2379–2400. https://doi.org/10.3390/ijgi4042379.
19. Wang, B.; Deveson, E.D.; Waters, C.; Spessa, A.; Lawton, D.; Feng, P.; Liu, D.L. Future Climate Change Likely to Reduce the Australian Plague Locust (Chortoicetes Terminifera) Seasonal Outbreaks. *Sci. Total Environ.* **2019**, *668*, 947–957. https://doi.org/10.1016/j.scitotenv.2019.02.439.
20. Clissold, F.J.; Simpson, S.J. Temperature, Food Quality and Life History Traits of Herbivorous Insects. *Curr. Opin. Insect Sci.* **2015**, *11*, 63–70. https://doi.org/10.1016/j.cois.2015.10.011.
21. Poniatowski, D.; Beckmann, C.; Löffler, F.; Münsch, T.; Helbing, F.; Samways, M.J.; Fartmann, T. Relative Impacts of Land-use and Climate Change on Grasshopper Range Shifts Have Changed over Time. *Glob. Ecol. Biogeogr.* **2020**, *29*, 2190–2202. https://doi.org/10.1111/geb.13188.
22. Prinster, A.J.; Resasco, J.; Nufio, C.R. Weather Variation Affects the Dispersal of Grasshoppers beyond Their Elevational Ranges. *Ecol. Evol.* **2020**, *10*, 14411–14422. https://doi.org/10.1002/ece3.7045.
23. Renier, C.; Waldner, F.; Jacques, D.; Babah Ebbe, M.; Cressman, K.; Defourny, P. A Dynamic Vegetation Senescence Indicator for Near-Real-Time Desert Locust Habitat Monitoring with MODIS. *Remote Sens.* **2015**, *7*, 7545–7570. https://doi.org/10.3390/rs70607545.
24. Stige, L.C.; Chan, K.-S.; Zhang, Z.; Frank, D.; Stenseth, N.C. Thousand-Year-Long Chinese Time Series Reveals Climatic Forcing of Decadal Locust Dynamics. *Proc. Natl. Acad. Sci. USA* **2007**, *104*, 16188–16193. https://doi.org/10.1073/pnas.0706813104.
25. Wysiecki, M.L.D.; Arturi, M.; Torrusio, S.; Cigliano, M.M. Influence of Weather Variables and Plant Communities on Grasshopper Density in the Southern Pampas, Argentina. *J. Insect Sci.* **2011**, *11*, 109. https://doi.org/10.1673/031.011.10901.
26. Humbert, J.-Y.; Delley, S.; Arlettaz, R. Grassland Intensification Dramatically Impacts Grasshoppers: Experimental Evidence for Direct and Indirect Effects of Fertilisation and Irrigation. *Agric. Ecosyst. Environ.* **2021**, *314*, 107412. https://doi.org/10.1016/j.agee.2021.107412.
27. Propastin, P. Satellite-Based Monitoring System for Assessment of Vegetation Vulnerability to Locust Hazard in the River Ili Delta (Lake Balkhash, Kazakhstan). *J. Appl. Remote Sens.* **2013**, *7*, 075094. https://doi.org/10.1117/1.JRS.7.075094.
28. Tian, H.; Stige, L.C.; Cazelles, B.; Kausrud, K.L.; Svarverud, R.; Stenseth, N.C.; Zhang, Z. Reconstruction of a 1,910-y-Long Locust Series Reveals Consistent Associations with Climate Fluctuations in China. *Proc. Natl. Acad. Sci. USA* **2011**, *108*, 14521–14526. https://doi.org/10.1073/pnas.1100189108.
29. Veran, S.; Simpson, S.J.; Sword, G.A.; Deveson, E.; Piry, S.; Hines, J.E.; Berthier, K. Modeling Spatiotemporal Dynamics of Outbreaking Species: Influence of Environment and Migration in a Locust. *Ecology* **2015**, *96*, 737–748. https://doi.org/10.1890/14-0183.1.

30. Leonard, A.; Egonyu, J.P.; Tanga, C.M.; Kyamanywa, S.; Tonnang, H.Z.E.; Azrag, A.G.A.; Khamis, F.M.; Ekesi, S.; Subramanian, S. Predicting the Current and Future Distribution of the Edible Long-Horned Grasshopper Ruspolia Differens (Serville) Using Temperature-Dependent Phenology Models. *J. Therm. Biol.* **2021**, *95*, 102786. https://doi.org/10.1016/j.jtherbio.2020.102786.
31. Leins, J.A.; Banitz, T.; Grimm, V.; Drechsler, M. High-Resolution PVA along Large Environmental Gradients to Model the Combined Effects of Climate Change and Land Use Timing: Lessons from the Large Marsh Grasshopper. *Ecol. Model.* **2021**, *440*, 109355. https://doi.org/10.1016/j.ecolmodel.2020.109355.
32. Fartmann, T.; Poniatowski, D.; Holtmann, L. Habitat Availability and Climate Warming Drive Changes in the Distribution of Grassland Grasshoppers. *Agric. Ecosyst. Environ.* **2021**, *320*, 107565. https://doi.org/10.1016/j.agee.2021.107565.
33. Branson, D.H. Effects of Altered Seasonality of Precipitation on Grass Production and Grasshopper Performance in a Northern Mixed Prairie. *Environ. Entomol.* **2017**, *46*, 589–594. https://doi.org/10.1093/ee/nvx053.
34. Buckley, L.B.; Graham, S.I.; Nufio, C.R. Grasshopper Species' Seasonal Timing Underlies Shifts in Phenological Overlap in Response to Climate Gradients, Variability and Change. *J. Anim. Ecol.* **2021**, *90*, 1252–1263. https://doi.org/10.1111/1365-2656.13451.
35. Kistner-Thomas, E.; Kumar, S.; Jech, L.; Woller, D.A. Modeling Rangeland Grasshopper (Orthoptera: Acrididae) Population Density Using a Landscape-Level Predictive Mapping Approach. *J. Econ. Entomol.* **2021**, *114*, 1557–1567. https://doi.org/10.1093/jee/toab119.
36. Li, L.; Zhao, C.; Zhao, X.; Wang, D.; Li, Y. Pattern of Plant Communities' Influence to Grasshopper Abundance Distribution in Heterogeneous Landscapes at the Upper Reaches of Heihe River, Qilian Mountains, China. *Environ. Sci. Pollut. Res.* **2022**, *29*, 13177–13187. https://doi.org/10.1007/s11356-021-16430-9.
37. Yadav, S.; Stow, A.; Dudaniec, R.Y. Elevational Partitioning in Species Distribution, Abundance and Body Size of Australian Alpine Grasshoppers (*Kosciuscola*). *Austral Ecol.* **2020**, *45*, 609–620. https://doi.org/10.1111/aec.12876.
38. Burt, P.J.A.; Colvin, J.; Smith, S.M. Remote Sensing of Rainfall by Satellite as an Aid to *Oedaleus Senegalensis* (Orthoptera: Acrididae) Control in the Sahel. *Bull. Entomol. Res.* **1995**, *85*, 455–462. https://doi.org/10.1017/S0007485300032922.
39. Ni, S.-X.; Wang, J.-C.; Jiang, J.-J.; Zha, Y. Rangeland Grasshoppers in Relation to Soils in the Qinghai Lake Region, China. *Pedosphere* **2007**, *17*, 84–89.
40. Ozment, K.A.; Welti, E.A.R.; Shaffer, M.; Kaspari, M. Tracking Nutrients in Space and Time: Interactions between Grazing Lawns and Drought Drive Abundances of Tallgrass Prairie Grasshoppers. *Ecol. Evol.* **2021**, *11*, 5413–5423. https://doi.org/10.1002/ece3.7435.
41. Zhou, W.; Wang, K.; Zhao, C.; Zhang, Q. Analysis of Spatial Pattern among Grasshopper and Vegetation in Heihe Based on GIS. *Phys. Procedia* **2012**, *33*, 1261–1268. https://doi.org/10.1016/j.phpro.2012.05.208.
42. Meynard, C.N.; Lecoq, M.; Chapuis, M.; Piou, C. On the Relative Role of Climate Change and Management in the Current Desert Locust Outbreak in East Africa. *Glob. Change Biol.* **2020**, *26*, 3753–3755. https://doi.org/10.1111/gcb.15137.
43. Ortego, J.; Aguirre, M.P.; Noguerales, V.; Cordero, P.J. Consequences of Extensive Habitat Fragmentation in Landscape-level Patterns of Genetic Diversity and Structure in the M Editerranean Esparto Grasshopper. *Evol. Appl.* **2015**, *8*, 621–632. https://doi.org/10.1111/eva.12273.
44. Lozano, F.J.; Suárez-Seoane, S.; Kelly, M.; Luis, E. A Multi-Scale Approach for Modeling Fire Occurrence Probability Using Satellite Data and Classification Trees: A Case Study in a Mountainous Mediterranean Region. *Remote Sens. Environ.* **2008**, *112*, 708–719. https://doi.org/10.1016/j.rse.2007.06.006.
45. Norberg, A.; Abrego, N.; Blanchet, F.G.; Adler, F.R.; Anderson, B.J.; Anttila, J.; Araújo, M.B.; Dallas, T.; Dunson, D.; Elith, J.; et al. A Comprehensive Evaluation of Predictive Performance of 33 Species Distribution Models at Species and Community Levels. *Ecol. Monogr.* **2019**, *89*, e01370. https://doi.org/10.1002/ecm.1370.
46. Padalia, H.; Srivastava, V.; Kushwaha, S.P.S. Modeling Potential Invasion Range of Alien Invasive Species, *Hyptis suaveolens* (L.) Poit. in India: Comparison of MaxEnt and GARP. *Ecol. Inform.* **2014**, *22*, 36–43. https://doi.org/10.1016/j.ecoinf.2014.04.002.
47. Farashi, A.; Kaboli, M.; Karami, M. Predicting Range Expansion of Invasive Raccoons in Northern Iran Using ENFA Model at Two Different Scales. *Ecol. Inform.* **2013**, *15*, 96–102. https://doi.org/10.1016/j.ecoinf.2013.01.001.
48. Lee, M.-J.; Kang, J.; Jeon, S. Application of Frequency Ratio Model and Validation for Predictive Flooded Area Susceptibility Mapping Using GIS. In Proceedings of the 2012 IEEE International Geoscience and Remote Sensing Symposium, Munich, Germany, 22–27 July 2012; IEEE: 2012; pp. 895–898.
49. Jebur, M.N.; Pradhan, B.; Tehrany, M.S. Optimization of Landslide Conditioning Factors Using Very High-Resolution Airborne Laser Scanning (LiDAR) Data at Catchment Scale. *Remote Sens. Environ.* **2014**, *152*, 150–165. https://doi.org/10.1016/j.rse.2014.05.013.

50. Shah, A.A.; Ullah, A.; Khan, N.A.; Shah, M.H.; Ahmed, R.; Hassan, S.T.; Tariq, M.A.U.R.; Xu, C. Identifying Obstacles Encountered at Different Stages of the Disaster Management Cycle (DMC) and Its Implications for Rural Flooding in Pakistan. *Front. Environ. Sci.* **2023**, *11*, 1088126. https://doi.org/10.3389/fenvs.2023.1088126.
51. Arabameri, A.; Pradhan, B.; Rezaei, K.; Lee, C.-W. Assessment of Landslide Susceptibility Using Statistical- and Artificial Intelligence-Based FR–RF Integrated Model and Multiresolution DEMs. *Remote Sens.* **2019**, *11*, 999. https://doi.org/10.3390/rs11090999.
52. Rehman, A.; Song, J.; Haq, F.; Mahmood, S.; Ahamad, M.I.; Basharat, M.; Sajid, M.; Mehmood, M.S. Multi-Hazard Susceptibility Assessment Using the Analytical Hierarchy Process and Frequency Ratio Techniques in the Northwest Himalayas, Pakistan. *Remote Sens.* **2022**, *14*, 554. https://doi.org/10.3390/rs14030554.
53. Dong, Z.; Zhang, J.; Tong, Z.; Han, A.; Zhi, F. Ecological Security Assessment of Xilingol Grassland in China Using DPSIRM Model. *Ecol. Indic.* **2022**, *143*, 109336. https://doi.org/10.1016/j.ecolind.2022.109336.
54. Yang, W.; Zhen, L. Household Perceptions of Factors That Affect Food Consumption in Grassland Areas: A Case Study in the Xilin Gol Grassland, China. *Environ. Res. Lett.* **2020**, *15*, 115007. https://doi.org/10.1088/1748-9326/abc0b9.
55. Jia, M.; Zhen, L. Food Consumption Characteristics and Influencing Factors in a Grassland Transect of Inner Mongolia Based on the Emergy Method. *Foods* **2022**, *11*, 3637. https://doi.org/10.3390/foods11223637.
56. Haiyan, D.A.I.; Haimei, W.A.N.G. Influence of Rainfall Events on Soil Moisture in a Typical Steppe of Xilingol. *Phys. Chem. Earth Parts A/B/C* **2021**, *121*, 102964. https://doi.org/10.1016/j.pce.2020.102964.
57. Zhang, N.; Zhang, H.-Y.; He, B.; Gexigeduren; Xin, Z.-Y.; Lin, H. Spatiotemporal Heterogeneity of the Potential Occurrence of Oedaleus Decorus Asiaticus in Inner Mongolia Steppe Habitats. *J. Arid. Environ.* **2015**, *116*, 33–43. https://doi.org/10.1016/j.jaridenv.2015.01.019.
58. Lu, L.; Kong, W.; Eerdengqimuge; Ye, H.; Sun, Z.; Wang, N.; Du, B.; Zhou, Y.; Weijun; Huang, W. Detecting Key Factors of Grasshopper Occurrence in Typical Steppe and Meadow Steppe by Integrating Machine Learning Model and Remote Sensing Data. *Insects* **2022**, *13*, 894. https://doi.org/10.3390/insects13100894.
59. Wang, F.; Chen, X.; Luo, G.; Ding, J.; Chen, X. Detecting Soil Salinity with Arid Fraction Integrated Index and Salinity Index in Feature Space Using Landsat TM Imagery. *J. Arid Land* **2013**, *5*, 340–353. https://doi.org/10.1007/s40333-013-0183-x.
60. Phillips, S.J.; Anderson, R.P.; Schapire, R.E. Maximum Entropy Modeling of Species Geographic Distributions. *Ecol. Model.* **2006**, *190*, 231–259. https://doi.org/10.1016/j.ecolmodel.2005.03.026.
61. Bujang, M.A.; Baharum, N. A Simplified Guide to Determination of Sample Size Requirements for Estimating the Value of Intraclass Correlation Coefficient: A Review. *Arch. Orofac. Sci.* **2017**, *12*, 1.
62. Phillips, S.J.; Anderson, R.P.; Dudík, M.; Schapire, R.E.; Blair, M.E. Opening the Black Box: An Open-source Release of Maxent. *Ecography* **2017**, *40*, 887–893. https://doi.org/10.1111/ecog.03049.
63. Huang, Y.; Dong, Y.; Huang, W.; Ren, B.; Deng, Q.; Shi, Y.; Bai, J.; Ren, Y.; Geng, Y.; Ma, H. Overwintering Distribution of Fall Armyworm (*Spodoptera frugiperda*) in Yunnan, China, and Influencing Environmental Factors. *Insects* **2020**, *11*, 805. https://doi.org/10.3390/insects11110805.
64. Rahman, Z.U.; Ullah, W.; Bai, S.; Ullah, S.; Jan, M.A.; Khan, M.; Tayyab, M. GIS-Based Flood Susceptibility Mapping Using Bivariate Statistical Model in Swat River Basin, Eastern Hindukush Region, Pakistan. *Front. Environ. Sci.* **2023**, *11*, 1178540. https://doi.org/10.3389/fenvs.2023.1178540.
65. Wan, G.-Z.; Wang, L.; Jin, L.; Chen, J. Evaluation of Environmental Factors Affecting the Quality of Codonopsis Pilosula Based on Chromatographic Fingerprint and MaxEnt Model. *Ind. Crops Prod.* **2021**, *170*, 113783. https://doi.org/10.1016/j.indcrop.2021.113783.
66. Ni, S.; Wu, T. *Monitoring the Intensity of Locust Damage to Vegetation Using Hyper-Spectra Data Obtained at Ground Surface*; Gao, W., Ustin, S.L., Eds.; San Diego, CA, USA, 2007; p. 66790B.
67. Sillero, N. What Does Ecological Modelling Model? A Proposed Classification of Ecological Niche Models Based on Their Underlying Methods. *Ecol. Model.* **2011**, *222*, 1343–1346. https://doi.org/10.1016/j.ecolmodel.2011.01.018.

Disclaimer/Publisher's Note: The statements, opinions and data contained in all publications are solely those of the individual author(s) and contributor(s) and not of MDPI and/or the editor(s). MDPI and/or the editor(s) disclaim responsibility for any injury to people or property resulting from any ideas, methods, instructions or products referred to in the content.